I. INTRODUCTION

MR diffusion tractography is a method for identifying white matter pathways in the living human brain. These pathways form the substrate for information transfer between remote brain regions and are therefore central to our understanding of function in both the normal and diseased brain. Tractography is the only available tool for identifying and measuring these pathways *non-invasively* and *in vivo*. By comparison with invasive techniques (Chapter 13), tractography measurements are indirect, difficult to interpret quantitatively, and error prone (Chapter 16). However, their non-invasive nature and ease of measurement mean that tractography studies can address scientific and clinical questions that cannot be answered by any other means. The following chapters will highlight many situations in which non-invasive measurements are essential in basic neuroscience and clinical research, and demonstrate their potential for surgery. In this chapter, we will outline the principles behind diffusion tractography.

All diffusion tractography techniques rely on one fundamental assumption: that, when a number of axons align themselves along a common axis, *the diffusion of water molecules will be hindered to a greater extent across this axis than along it*. Hence, when we measure diffusion along many different orientations, we expect to see diffusion *preferred* in orientations that correspond to axonal fiber orientations. This assumption is explained and investigated in detail in other chapters in this book but, throughout the complexities in the remainder of this chapter, it is crucial to remember the fundamental measurement that all of our inference relies upon. In attempting to reconstruct fiber bundles or draw inferences about axonal connectivity, tractography algorithms aim to find paths through the data field along which *diffusion is least hindered*.

While this fundamental objective is common throughout diffusion tractography, strategies for achieving it vary greatly from algorithm to algorithm. Tractography algorithms can be local or global, deterministic or probabilistic, model based or model free; they can rely on simple or complex representations of diffusion in white matter. Each of these different decisions (and several more subtle ones) impacts on the interpretation of the reconstructed white matter pathways and connectivity indices. Here, we review these techniques and examine their implications.

II. STREAMLINE TRACTOGRAPHY

Tractography is the process of *integrating* voxel-wise fiber orientations[1] into a pathway that connects remote brain regions. As you will see later in the chapter, this integration can be achieved in different ways, but it is useful first to consider the most intuitive and most commonly used: the streamline.

A. The Streamline

A streamline through a vector field is any line whose tangent is always parallel to the vector field. Such streamlines are the intuitive method for performing tractography as they can be reconstructed by simply starting at a seed point and following the local vector information on a step-by-step basis, effectively "joining the arrows". The process is easy to imagine, and can be seen in Figure 15.1. While this intuitive explanation is clearly helpful, it is also beneficial to consider a mathematical representation of a streamline, as this representation raises key issues that will recur throughout the different tractography approaches.

Mathematically, a streamline can be represented as a 3D space-curve, as described in Basser *et al.* (2000) (see Figure 15.1b). The equation describing the curve derives from the fact that the tangent to the streamline must be parallel with the fiber orientation. The location of the streamline, $\mathbf{r}$, is a function of the arc length s (the distance along the streamline from the start). In order for the streamline to trace fiber trajectories through the vector field, the tangent to the streamline at arc length s is taken to be the local estimate of fiber orientation. Assuming, for now, that we are relying on the diffusion tensor model (see Chapter 3) to obtain local fiber orientations, this tangent is assumed to be the first eigenvector of the diffusion tensor, i.e. $\mathbf{t}(s) = e_1(\mathbf{r}(s))$, where $\mathbf{r}(s)$ is the $[x, y, z]$ location that is distance s along the streamline. The mathematical equation describing the evolution of a streamline through the data is therefore (Basser *et al.*, 2000):

$$\frac{d\mathbf{r}(s)}{ds} = \varepsilon_1(\mathbf{r}(s)) \qquad (15.1)$$

[1] Note, for the remainder of the chapter we will often refer to fiber orientation rather than principal diffusion orientation to account for models that allow for more than one fiber orientation (see Chapter 4 and later sections in this chapter). It is of course important to remember that this terminology encompasses the assumption that fiber orientations align with orientations of maximal diffusion.

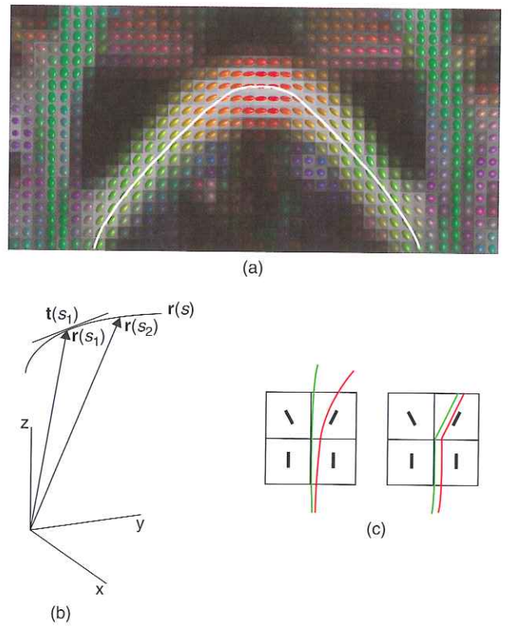

FIGURE 15.1 Streamline tractography. (a) shows streamline tractography from a conceptual perspective. The white streamline follows the orientations of least hindrance to diffusion (here the principal axes of diffusion tensors). (b) shows a mathematical representation of streamline tractography. The streamline location is parameterized as a vector $\mathbf{r}$ which is a function of length along the streamline s. The tangent to the streamline $\mathbf{t}(s)$ is the estimate of local fiber orientation. (c) shows the effect of two common forms of interpolation on tractography. In the left panel the original *data* are interpolated in a linear fashion. In the right panel the fiber orientations are interpolated according to their nearest neighbors as in FACT (Mori *et al.*, 1999).

It is worth explaining here that equation (15.1) is a *differential equation*. This means that we do not have an equation that allows us to calculate directly the *location* of the streamline at any point along its arc (i.e. $\mathbf{r}(s)$). Instead we have an equation describing how this location should *change* (i.e. $d\mathbf{r}(s)/ds$). Crucially, this implies that any errors in our calculations of the streamline will be *compounded* as the streamline progresses. However, it also allows us to draw on a large literature describing the evolution of these errors in differential equations, and strategies for minimizing them (see later).

1. *Interpolation*

The second important feature to take from equation (15.1) is that the equation's right-hand side is defined in continuous space. That is, if we want to know how the streamline should progress from its location $\mathbf{r}(s)$, we need to know the local fiber orientation at this exact location. Unfortunately, the diffusion data that the local fiber orientations are derived from are acquired on an imaging grid. Hence, we only have one measurement of orientation in every imaging voxel. We therefore need a method of "guessing" from the gridded data what the fiber orientation measurement would have been at locations away from the voxel centers, i.e. we need a method for *interpolating* our discrete measurements into continuous space. Different streamline tractography tools take different approaches to the interpolation problem (see Figure 15.1c). For example, early techniques (Mori *et al.*, 1999) assumed that the measurement from each voxel should be applied over the entire voxel (Figure 15.1c right). It has been shown (Lazar and Alexander, 2003) that such an assumption leads to a greater propagation of errors in tractography than approaches that perform a *smooth* interpolation between grid points (Figure 15.1c left). In smooth interpolation approaches, assumed fiber orientations between grid points contain contributions from each neighboring point. This can be achieved by combining either the original data, or the derived diffusion profiles (Pajevic *et al.*, 2002) from points on the measurement grid.

2. In vivo *Dissection*

Perhaps the greatest success in tractography to date is the use of streamline tractography for *in vivo dissection* (e.g. Stieltjes *et al.*, 2001; Catani *et al.*, 2002). Here, the goal is to isolate and delineate major white matter pathways in individual human brains (Figure 15.2a). The technique relies on the streamline tractography principles outlined above, and supplements them with prior anatomical knowledge of the trajectories of major fiber bundles in the brain. Streamlines are seeded from every voxel in the brain, but only retained if they meet anatomical criteria. Streamlines are required to pass through (usually two) white matter regions of interest that uniquely define known pathways (Figure 15.2b). This technique has been successfully deployed to isolate and visualize many different white matter pathways. For example, Figure 15.2a shows a successful 3D reconstruction of some of the major white matter bundles using streamline tractography. The figure shows, among other tracts, the trajectories of the arcuate fasciculus, corona radiata, uncinate fasciculus (sagittal view), as well as the corpus callosum and many short association fibers (axial

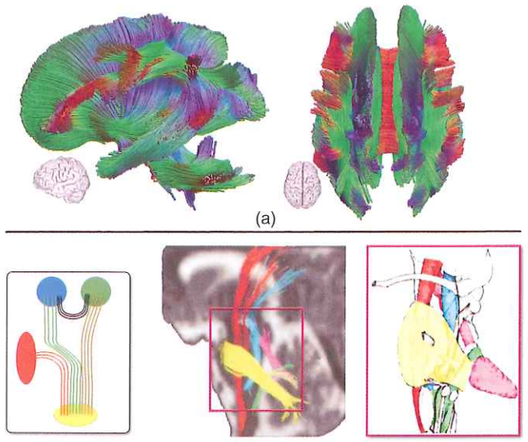

FIGURE 15.2 Examples of virtual dissections of human white matter tracts. (a) Sagittal – left – and axial – right – views showing 3D reconstructions of white matter pathways using streamline tractography. Major tracts are depicted, such as the corona radiata, arcuate, and uncinate fasciculus (left) and corpus callosum (right). Image courtesy: Alexander Leemans. (b) Example tracking of pathways within the brainstem using streamline tractography combined with anatomically meaningful regions of interest. Restricting the tractography to pathways that reach given pairs of regions allows one to delineate the cortico-spinal tract (red), medial lemniscus (green), and inferior (yellow), medial (cyan) and superior (pink) cerebellar peduncle. The results of the tractography show a high degree of resemblance with a hand drawing of the anatomy of those pathways. Modified with permission from Stieltjes *et al.* (2001).

view). The level of details achieved by this technique qualitatively matches the results of white matter dissection studies (Lawes *et al.*, 2008).

However, tractography is of value for more than just visualization. By providing tools for segmenting the white matter into functionally distinct pathways, *in vivo* dissection techniques allow unbiased, anatomically meaningful regions of interest to be identified in individual brains. As is discussed in detail in Chapter 8, such ROIs can then be used to provide quantitative measurements (e.g. FA) for comparison across subjects or groups (e.g. Gong *et al.*, 2005; Ciccarelli *et al.*, 2006; Jones *et al.*, 2006). Such an approach not only solves the correspondence problem of matching similar regions across different subjects, but also provides functionally relevant ROIs for signal averaging (see Chapter 8).

3. Errors in Streamline Tractography

Despite the success of *in vivo* dissection techniques in segmenting and visualizing major white matter pathways, any tractography process is susceptible to

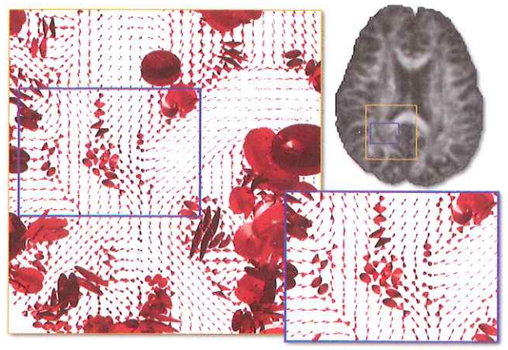

FIGURE 15.3 Cones of uncertainty calculated using the bootstrap technique. Top right: Fractional anisotropy map. The magnified region in orange shows the 95% uncertainty cones within a region of the splenium of the corpus callosum. The further magnified region in blue shows a location where white matter bundles cross, producing a high degree of uncertainty on the PDD. Image courtesy: Derek Jones.

errors. The causes of such errors can be separated into three major categories:

1. Imaging noise causing poor estimation of dominant diffusion directions.
2. Modeling error, resulting from the microscopic anatomy of the white matter being more complex than can be represented by the choice of model (for example, the diffusion tensor model cannot represent regions where fiber bundles cross).
3. Integration errors introduced in the tractography process.

As we show below, errors in streamline-based tractography approaches *accumulate* along the streamline. It is therefore easy to imagine each of these error sources having a catastrophic effect on reconstructed pathways. However, it is also easy to see that these effects are likely to depend on the particulars of the white matter anatomy in the region where the errors are introduced. Figure 15.3 shows empirical measurements of the errors introduced by imaging noise and modeling error on the estimation of the principal diffusion direction. Jones (2003) acquired two apparently identical measurements in each of 64 diffusion encoding directions. He then created 1000 different data sets by *bootstrapping*. For each new data set he selected one of the two measurements at random at each orientation and each slice. He then reconstructed diffusion tensors, and principal diffusion directions in each of the bootstrapped data sets. Each voxel in Figure 15.3 displays the 95% confidence cone for this principal diffusion direction. The width of these cones therefore represents the uncertainty in PDD caused by errors

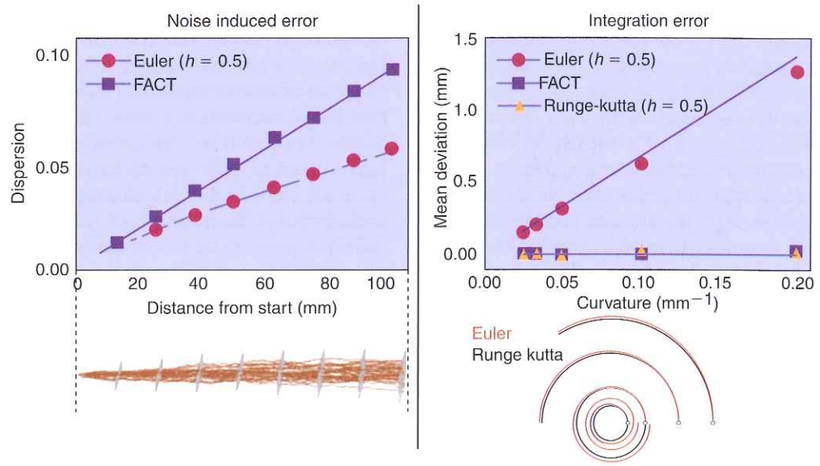

FIGURE 15.4 Analysis of the effect of noise and integration error on streamline tractography. Left panel: Dispersion of the tracts along a linear noisy tensor map using Euler integration method and FACT, a method that does *not* interpolate the local orientations. Right panel: Mean deviation of the reconstructed pathways from the true solution along noiseless circular tensor fields with increasing curvature. Overall, the Runge–Kutta method, combined with interpolation of the tensors, is the most accurate both in terms of integration error and minimization of the compounded effect of noise. Modified from Lazar and Alexander (2003).

in the measurement and modeling processes. A quick examination of the figure reveals that such errors can indeed be large, but also gives some insight into the success of the *in vivo* dissection techniques described above. Errors are largest in gray matter and CSF. In the white matter, the largest errors occur as pathways approach cortex or at junctions between white matter pathways, where more than one fiber bundle may exist within a voxel. In the deep white matter that is crucial for the reconstruction of major pathways, errors are small.

Lastly, streamline tractography is subject to integration errors. In order to understand this last point, let us return to the mathematical representation of a streamlining process, i.e. as a differential equation of the form $d\mathbf{r}(s)/ds = f(s,\mathbf{r})$. This equation is written in the continuous space, meaning that $(s, f, \mathbf{r})$ vary continuously. However, f is effectively measured on a discrete grid (e.g. voxelwise principal diffusion direction), and the derivative of $\mathbf{r}$ needs to be discretized in order to be solved numerically. These approximations inevitably lead to errors that accumulate along the streamline. There are two choices to make for the design of a numerical method for streamlining: (1) how to interpolate f and (2) how to discretize $d\mathbf{r}(s)/ds$? We have already presented the options for (1). Techniques for discretizing $d\mathbf{r}(s)/ds$ generally consist of transforming it into the finite difference $(\mathbf{r}(s + h) - \mathbf{r}(s))/h$, i.e. approximating a continuous *derivative* by a difference along a small step size h. The value of f may be assumed constant during that step size (Euler method) or, more accurately, variations of f between $\mathbf{r}(s)$ and $\mathbf{r}(s + h)$ may be taken into account (Runge–Kutta). Again, despite all care in descritizing this derivative, errors will always be compounded along the streamline. However, integration errors diminish with decreasing step size and increasing account higher-order variations of f. Furthermore, there are possibilities for quantifying, or at least calculating theoretical bounds, for the local and/or accumulated error.

Choices of either strategy have different implications. Figure 15.4 shows simulations that illustrate the outcome of each choice (taken from Lazar and Alexander, 2003). It also shows that combining a continuous interpolation of f with the Runge–Kutta method is best for minimizing both integration error and the compounded effect of noise.

4. When to Stop a Streamline

If errors exist in the tractography process, and cause failures in the reconstruction of accurate streamlines, it then becomes important to develop an understanding of when a streamline should and should not be trusted, and therefore when a streamline should be stopped. Streamline tractography as described above has no mechanism for determining *confidence* in the next step as the streamline progresses, and therefore

no mechanism with which to estimate the confidence or uncertainty in the location of the streamline at each point along its length. Nevertheless, because of the accumulation of errors along a streamline, there is inherent uncertainty associated with each streamline location. Because of the lack of a formal representation of this uncertainty, streamline tractography must rely on heuristic rules that stop the streamline when it reaches a point where high uncertainty is expected.

The two most common heuristics applied to stop the streamline are an *FA threshold* and a *curvature threshold*, and they are used for different reasons. A quick re-examination of Figure 15.3 immediately shows the rationale for the *FA* threshold: Regions of low FA tend to be associated with high uncertainty in principal diffusion direction (large 95% confidence cones), and therefore large potential error for the next streamline step. Hence, by stopping the streamline whenever the FA falls below a threshold value, it is possible to minimize the chances of the streamline encountering large errors along its path. The curvature threshold, as its name implies, imposes a maximum curvature (often measured as the angle between two successive steps) permissible along the streamline. The rationale for this heuristic comes from the anatomy of the white matter in major white matter pathways. It is unusual to find bends in such pathways that have radii of curvature on the scale of an imaging voxel (i.e. it is unusual to find pathways that bend through a large angle in only a few millimeters). Hence, if a streamline encounters a particularly large angle between two successive steps or, almost equivalently, a particularly small radius of curvature, it is more likely to be caused by erroneous measurement than by such a bend existing in underlying white matter trajectory.

III. PROBABILISTIC TRACTOGRAPHY

As we saw at the end of the last section, the data and modeling upon which tractography relies are subject to errors, and these errors propagate through the tractography process, potentially leading to erroneous statements about white matter connectivity. The goal of probabilistic tractography is, instead of simply stopping tractography in regions and along trajectories in which such errors are likely, to develop a full representation of the *uncertainty* associated with any eventual statement that might be made. Probabilistic tractography aims to make the following statement:

> Given the model and the data, I have x% confidence that the path of least hindrance to diffusion from seed point A passes through region B.

By treating the problem in this fashion, probabilistic tractography techniques are able to track through regions of high uncertainty, where *deterministic* techniques (such as streamlining) would be forced to stop, but they acknowledge that statements that can be made about anatomical locations beyond this uncertain region must be made with lower confidence (x) or about a larger target brain region (B). Furthermore, probabilistic tractography techniques allow the user to quantify and compare the confidence that the error-free streamline from any one region might reach any of a number of different target regions. It is perhaps already becoming clear that these statements and comparisons are not exactly the ones that anatomists would like to make (see later section II.K). However, it is also clear that the statements and comparisons that can be made are both more complete, and more flexible than is the case with deterministic approaches.

A. Characterizing Uncertainty

The first step in any probabilistic tractography technique is to build a function that characterizes the uncertainty in our key measurement, the fiber orientation.[2] This function is an orientational density function (ODF) that describes the probability density on the true fiber orientation. In keeping with Chapter 4, we will refer to this as the *uncertainty ODF* (the uODF).

1. The uODF and Other Less Confusing ODFs (See Chapter 4)

An orientation density function can be imagined as a sphere whose surface value changes as a function of latitude and longitude (for example, average rainfall on the world's surface). There are three ODFs that are important to understand, and to dissociate in diffusion tractography – the diffusion ODF (dODF), the fiber ODF (fODF), and the uncertainty ODF (uODF). The first two of these ODFs are described and depicted in detail in Chapter 4 but we overview them conceptually here for comparison with the uODF.

The dODF and the fODF both describe biophysical properties of the tissue that is being measured, but at different levels. The fODF is both the most intuitive and the most biologically relevant. It describes the proportion of fibers that lie along each orientation.

[2] Again, it is important to remember that the measurement is of orientations of maximal diffusion and the link to fiber orientation is an empirical approximation.

For example, a voxel that contains two perpendicular fiber bundles each containing perfectly aligned fibers will have an fODF in the shape of a cross, but if each of these bundles has some misalignment in its constituent fibers, then the peaks of the fODF will bulge at the ends (e.g. Tournier *et al.*, 2004). With the exception of some ambiguities in fiber structure that are discussed in Chapter 4, the fODF then contains exactly the information that is needed to estimate a biophysically meaningful measure of connectivity: the proportion of fibers leaving region A that reach region B. However, because our measurement probe is the diffusion of water molecules, unfortunately the fODF cannot be measured directly. Instead, our measurements are a function of the dODF. The dODF describes the orientational structure of *diffusion* in the voxel (e.g. see Tuch *et al.*, 2003). More formally it describes the probability, after a diffusion time τ that a spin will have moved along any particular orientation from its position at the start of the experiment. If water molecules could only move along the fiber orientation, then the dODF should be identical to the fODF. However, although diffusion is thought to be least hindered along fiber orientations, there is still a significant component of diffusion along other orientations, even perpendicular to this main fiber axis. The result of this is that the dODF is necessarily *much* broader than the fODF.

Unlike the dODF and the fODF, the *uncertainty* ODF (uODF) is not a physical property of the system that is being measured. Instead, it is a function that describes our *belief*. As in every situation in which the goal is to infer useful information from noisy data, when we are trying to infer major fiber orientations, or dODFs or fODFs from diffusion MRI data, we encounter uncertainty. We can never be confident in the exact orientations, probabilities, or fiber proportions we measure. The uODF characterizes this uncertainty by representing our confidence that the true parameter of interest (for example, a fiber orientation) lies within any particular area on the surface of the sphere. The 95% cones of uncertainty seen in Figure 15.3 are a good example of key features that are represented by a uODF. Here the orientational widths that are spanned by 95% of the density of the uODF are represented graphically as cones. These cones do not represent the spread of fibers in a voxel, nor the possible trajectories of water molecules in a diffusion time. Instead they represent a statement about our confidence in our measurement of the principal diffusion direction. In order to assess the confidence we can have in our final assessment of anatomical connectivity, it is clear that we must be able to represent our confidence in our initial measurements of fiber orientation.

2. Calculating uODFs

(Ignore this section if you are not interested in the maths.)

a. Bootstrapping

In Figure 15.3 we have already seen perhaps the most intuitive method for constructing the uODF, we can simply take multiple repetitions of the original data, reconstruct our measure of interest (here the principal diffusion direction) in each data set, and treat these repeated measurements as *samples* from the uODF (Jones, 2003). As will be seen later, it is often the case that such *samples* are exactly what are needed to propagate the uncertainty to tract solutions in probabilistic tractography but, if needed, a full representation of the uODF can be constructed from many such samples by binning them to form a spherical histogram. Because many samples are required to build a good representation of the uODF, and because it is not practical to acquire a large number (50–1000) of independent data sets (each data set takes perhaps half an hour to acquire) such multi-acquisition approaches rely on *bootstrapping* from a small number of original data sets (Jones, 2003). As we have described above, this is possible because each data set contains measurements along a number of different gradient orientations (here 64). Hence, it is possible to create many new data sets by, each time, choosing each of the 64 orientations from one of the four original data sets at random (Figure 15.5a). For example, we might end up with one new data set whose first orientation is taken from data set 3, whose second orientation is taken from data set 1, etc. Such *data bootstrapping* approaches compute the uODF making very few assumptions, but have two clear drawbacks. First, they impose a large load on the data acquisition. For example, the data in Figure 15.3 required two repeats of the data in order to characterize the uODF (although the schematic representation in Figure 15.5 uses three repeats). Second, each of the bootstrapped data sets is derived from the same two original data sets. This means that the bootstrapped data sets are not *independent samples*, leading to an underestimate in the estimate of uncertainty.

These two drawbacks are addressed explicitly by the use of the *WILD bootstrap* (Jones, 2008; Whitcher *et al.*, 2008), at the expense of some simple assumptions about the noise structure in the data. Here, instead of bootstrapping independent original data sets to make sample data sets, only a single original data set is required. When we fit a local diffusion model (for example, the diffusion tensor) to this data set, the predicted signal will not fit the data precisely (due to image noise and modeling error). The difference